ISBN: 978-3-95450-194-6 ISSN: 2226-0366 doi:10.18429/JACoW-LINAC2018-FR1A01

RESULTS FROM THE 6D DIAGNOSTICS TEST BENCH AT SNS

B. Cathey, A. Aleksandrov, S. Cousineau, A. Zhukov
Oak Ridge National Laboratory, Oak Ridge, TN, USA

Abstract

This paper presents the method and results for measuring the full six-dimensional phase space of a low energy, high intensity hadron beam. This was done by combining four-dimensional emittance measurement techniques along with dispersion measurement and a beam shape monitor to provide the energy and arrival time components. The measurements were performed on the new Beam Test Facility (BTF) at the Spallation Neutron Source (SNS), a 2.5 MeV functional duplicate of the SNS accelerator front end. The results include a correlation the had not previously been observed.

INTRODUCTION

For high power, high intensity accelerators, beam loss is one of the limiting factors for performance and achievable beam power [1]. Today's state-of-the-art simulation codes provide accurate tracking for the RMS values of the beam through the beam line for many cases, and in principle should also be able to accurately track the beam halo formation and beam loss through the accelerator. However, successful simulation of beam halo and beam loss have yet to be accomplished. As the capabilities of the simulations should be sufficient, the problem may then lie in an incorrect initial assumption, and the most likely candidate is the initial particle distribution, as it is generally approximated [2].

In order to determine the initial particle distribution, the beam must be measured over all six independent spatial and momentum parameters in such a way that correlations between parameters can be seen. The Beam Test Facility at SNS is a small-scale accelerator that can accomplish this task [3].

EMITTANCE MEASUREMENT

Typically, three separate two dimensional phase space measurements are combined to create a six dimensional distribution. However, because the un-measured cross-terms are assumed to be zero in this reconstruction, this distribution may not be identical the actual six dimensional distribution. In order to determine true six dimensional distributions, all six degrees of freedom must be directly measured together. The technique used here is a generalization of the two-dimensional phase space measurement method using slits and a charge collector for the complete six-dimensional phase space.

The particles go through a series of five apertures and a Beam Shape Monitor (BSM). Each aperture allows particles through at the coordinate being measured. By combining two pairs of apertures, one pair being horizontal slits and the other pair vertical slits, the four-dimensional transverse phase space is measured.

To select the longitudinal momentum, we use a 90-degree bending magnet. During the turn, the beam spreads as higher momentum and lower momentum particles separate horizontally due to dispersion. This creates a correlation between the horizontal position and the longitudinal momentum of a particle allowing the selection of particles with certain momentum based on their horizontal position. This selection is executed using a third movable vertical slit.

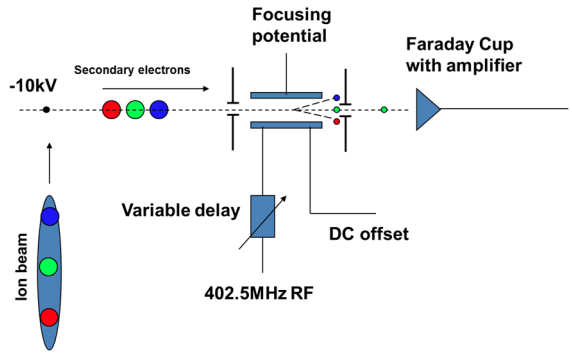

Figure 1: A diagram of the basic concept behind the BSM for measuring the longitudinal phase distribution in the beam.

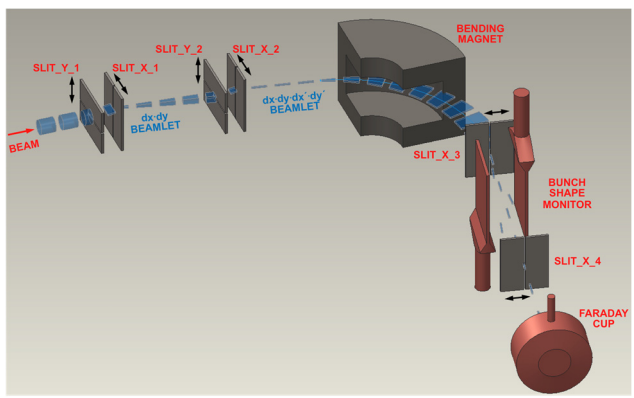

Figure 2: A diagram showing the concept of a full six-dimensional emittance scan.

The longitudinal measurement is conducted with a Beam Shape Monitor (BSM). The BSM contains a suspended wire with a potential in the beam pipe. When the hadron beam hits the wire, electrons are emitted which travel through a RF field and final aperture. See Fig. 1 and [3] for more details. These electrons then hit a detector and are measured as current. This final current measurement reflects the number of particles in the beam with the six measurements described above, particles with a specific horizontal, vertical, and longitudinal position and momentum. Figure 2 shows the full conceptual schematic for the six-dimensional measurement. After a measurement is made for a specified arrangement of apertures, one aperture is moved to the next position. This

ISBN: 978-3-95450-194-6 ISSN: 2226-0366 doi:10.18429/JACoW-LINAC2018-FR1A01

continues until all the wanted coordinates had been measured.

A modification to the above plan is the use of scintillating screens. A screen can measure an entire dimension at once to greatly reduce scan time. Two screens were installed in the BTF. The first is the energy slit, which can be seen in Fig. 3. The second replaces the aperture and Faraday cup after the deflector inside the BSM. Because using a screen blocks the beam, the energy screen cannot be used for a full six-dimensional scan as the beam cannot reach the BSM. As the beam travels through slits for select coordinates, a large fraction of particles is lost. By the end, approximately 10^{-7} of the particles from the original beam core reach the detector. This is sufficient for five-dimensional scans but not for six-dimensional scans using the BSM screen. As such, a micro-channel plate (MCP) is used to increase the signal strength for the BSM screen.

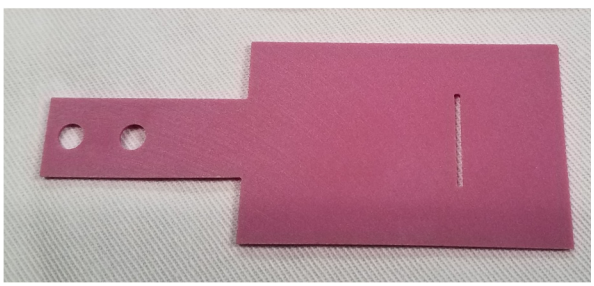

Figure 3: The Energy (fifth) slit that also doubled as a scintillating screen.

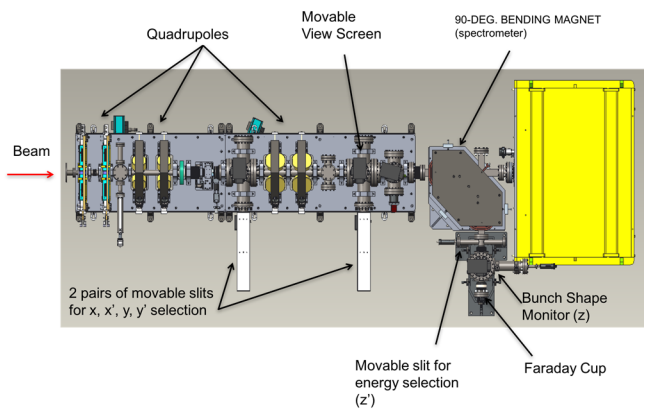

Figure 4: A schematic view of the BTF section where the diagnostics for the six-dimensional scan occur.

The Beam Test Facility (BTF) at the Spallation Neutron Source (SNS) houses the experiment [4]. Figure 4 shows the beam line downstream of the RFQ where the diagnostics are located. After the RFQ, there are four quadrupole magnets for focusing followed by two moveable slits, one aligned on the horizontal and the other on the vertical. The third pair of quadrupoles is followed by the second pair of identical slits. These slits all have an aperture width of 200 μm. Next is the 90^0 bend using a dipole magnet, followed by a final moveable aperture aligned vertically. The beam line ends at the Beam Shape Monitor. Specialized scripts based on an Open XAL framework were developed and are used to perform the multidimensional scans [5].

DATA ANALYSIS

After a scan is made, it is necessary to interpolate the raw data because it is rarified and not on a regular grid. Interpolating to a regular grid allows for quick integration over dimensions to view subsets of the data and helps generate more realistic distributions for simulations. However, interpolating so many points in six dimensions is complicated.

Custom codes were written to take advantage of how the data is saved. A linear interpolation method is shown in Fig. 5 for a six-dimensional scan. The logic is to interpolate one dimension at a time in the order the measurements are made, starting by interpolating over the set of x points for each different set of (y, x', y', w). This is done by interpolating the phase plots point by point linearly to determine the phase plot at new regular x points. The result is a regular 2D grid for each set of (y, x', y', w) of x and phase. This technique continues for each dimension, interpolating point by point for increasing dimensionalities, using the same order as the scan until a regular 6D space is built. Once the data has been interpolated, correlations can be found quicker and distributions can be generated for simulations.

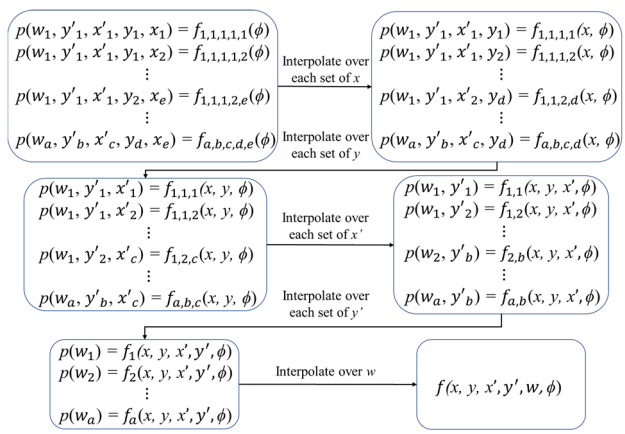

Figure 5: Scheme for 6D interpolations.

Many measurements, including the first full six-dimensional scan, were completed using the technique described above. The six-dimensional scan took 32 hours and resulted in 5,675,740 points on a near-regular grid in the 6D phase space. Figure 6 shows that the beam current during the 6D scan, measured upstream of the slits, remained constant for the duration except for a few dropouts. The experimental data provide an opportunity to explore the internal structure of the full phase space distribution, and specifically to check for correlations between coordinates in all six degrees of freedom. There is no proven technique for finding arbitrary correlations in high dimensional spaces. The linear correlation coefficients can be calculated for all combinations of the six degrees of freedom, but even zero values for the correlation coefficients do not guarantee the absence of

ISBN: 978-3-95450-194-6 ISSN: 2226-0366 doi:10.18429/JACoW-LINAC2018-FR1A01

higher order correlations, and a correlation of any order invalidates the common assumptions for the 6D phase space. Full exploration of this problem remains to be done.

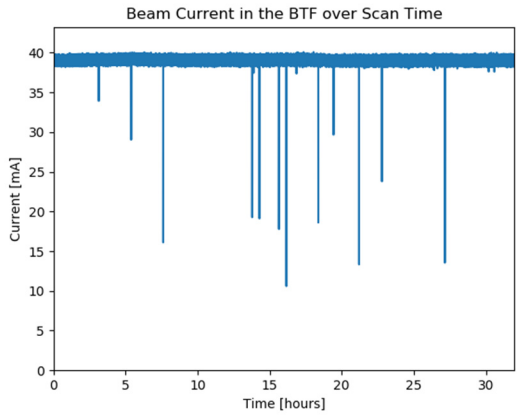

Figure 6: The beam current upstream of the slits measured during the 6D scan.

In order to visually show possible correlations within the distributions, a method of displaying the 6D results in 2D is needed. This is done through various 1D and 2D projections and partial projections of the higher dimension distributions. The key advantage of using the partial projections is that they avoid integration over all dimensions, which can mask important details of the high dimensionality distribution. The following definitions are used in the data analysis discussion below. Full projections are reduced dimensionality distribution functions obtained by integrating over all unused coordinates:

1D: $$f(a) = \int_{-\infty}^{\infty} f_6(a, \vec{x})\, d\vec{x},$$

2D: $$f(a,b) = \int_{-\infty}^{\infty} f_6(a, b, \vec{x})\, d\vec{x}.$$

On the other hand, partial projections are reduced dimensionality distribution functions obtained by fixing some coordinates to constant values and integrating over others:

1D: $$p(a) = \int_{-\infty}^{\infty} f_6(a, \vec{v} = \overrightarrow{v_0}, \vec{x})\, d\vec{x},$$

2D: $$p(a,b) = \int_{-\infty}^{\infty} f_6(a, b, \vec{v} = \overrightarrow{v_0}, \vec{x})\, d\vec{x}.$$

In the formulas above a, b are any coordinate from $(x, x', y, y', w, \varphi)$ set; $\vec{v}$ is a vector of coordinates remaining in $(x, x', y, y', w, \varphi)$ set after a, b are removed; $\vec{x}$ is the vector of coordinates remaining in $(x, x', y, y', w, \varphi)$ set after a, b and $\vec{v}$ are removed. Vector $\vec{v}$ is equal to the vector $\vec{v}_0$, which is the fixed coordinate of interest for the partial projection. A partial projection can be measured directly by leaving the selectors responsible for the fixed coordinate $\vec{v}_0$ at fixed positions during a scan. These scans are much faster than full 6D scans and allow exploring spaces of interest with higher resolution. Multiple scans with different beam parameters can also be done this way in reasonable time durations.

RESULTS

Below are some results from past scans. Figure 7 shows a one-dimensional scan that used a single slit to measure the horizontal beam distribution and the one-dimensional horizontal axis projection from a four-dimensional scan. Note the agreement is very good. Figure 8 is the two-dimensional horizontal phase space component of a five-dimensional scan measurement. And Figure 9 shows the two-dimensional distribution of vertical momentum against horizontal position projected from the same five-dimensional scan.

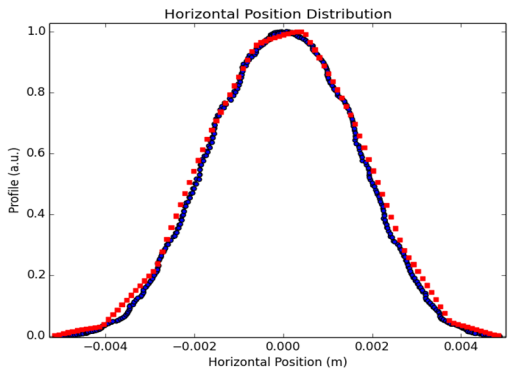

Figure 7: The horizontal beam distribution. Blue is directly measured with a single slit. Red is the projection from a 4D measurement.

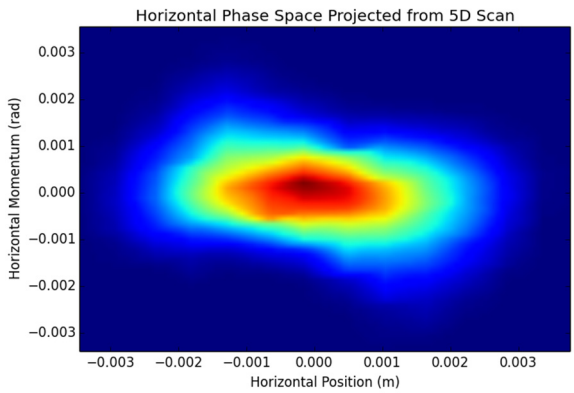

Figure 8: The horizontal phase space from a 5D measurement.

An interesting result was found using five-dimensional scans. Figure 10 shows a 2D color map of the $p(x',w)$ partial projection with $x = y = y' = 0$ (these slits were fixed in the beam center while the x' slit was allowed to move) and integrated over φ (the energy screen was used). A dependence of the w distribution upon the coordinate value x' is obvious in the plot. The w distribution showed similar dependence with x, y, and y' as well. Figure 11 is a graph of the energy spread for an entire 5D scan projected to a single dimension, showing the expected distribution peaking at the target energy.

ISBN: 978-3-95450-194-6 ISSN: 2226-0366 doi:10.18429/JACoW-LINAC2018-FR1A01

Figure 12, in turn, shows the graph of selected energy spreads measured near the beam core. These are individual measurements with the transverse position and vertical momentum all located at the beam center, but with three different horizontal momenta. The blue curve is where the horizontal momentum is zero. Two peaks with a dip at the reference energy are observed. This result was only found at the beam core; the measured distribution was Gaussian as expected farther away from the center. Figure 13 shows a partial projection of the longitudinal phase space where the transverse slits were all arranged to allow the center of the beam through, $x = y = x' = y' = 0$. This measurement represents a single part of a full 6D measurement. The distribution shows the expected linear correlation between energy and phase with the two peaks seen in the previous figures.

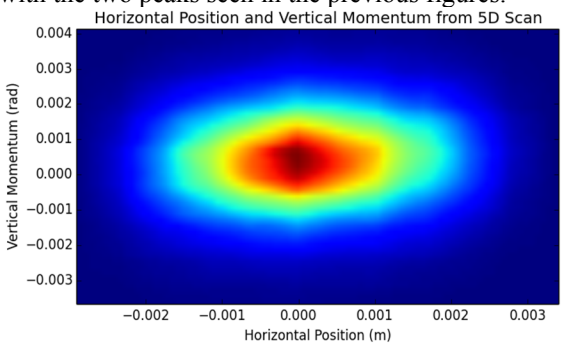

Figure 9: Vertical momentum versus horizontal position distribution from a 5D measurement.

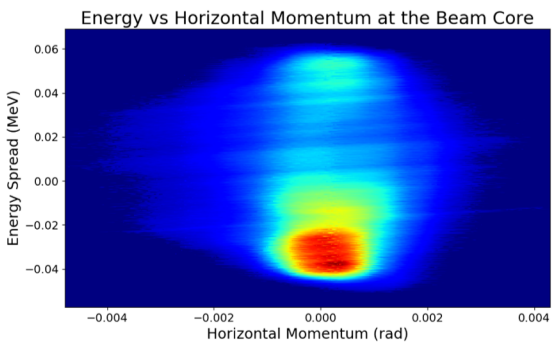

Figure 10: The energy spread from a 5D scan

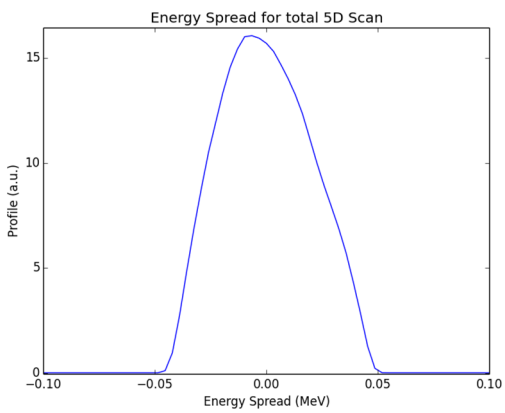

Figure 11: The energy spread from a 5D scan.

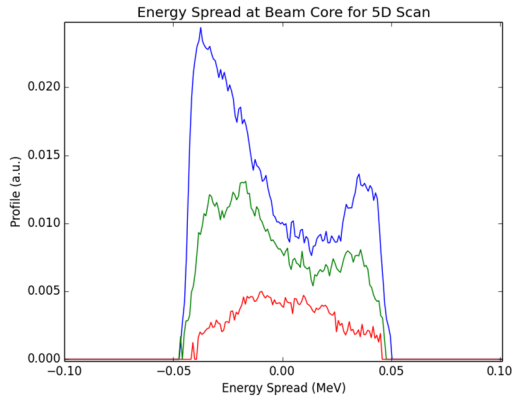

Figure 12: Energy spread from beam core in 5D scan. Blue is with no horizontal momentum. Green and red have horizontal momenta progressively further from zero.

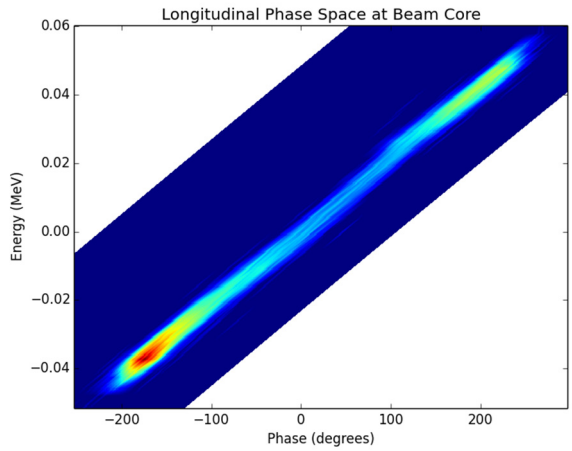

Figure 13: The longitudinal phase space measured at the beam core.

The plots in Fig. 14 show 1D partial projection energy spectrums with different numbers of fixed coordinates: the green line shows the energy spectrum measured with $x = x' = 0$ and integrated over y, y'; the red line shows the energy spectrum measured with $x = x' = y = 0$, integrated over y'; and the blue line shows the energy spectrum measured with $x = x' = y = y' = 0$. All three measurements are integrated over φ. The plots demonstrate the necessity of performing the scan in at least 4D for the correlation to become visible, and in 5D for resolving the details. The plots in Fig. 15 show 1D partial projections with four fixed coordinates $x = x' = y = y' = 0$ (all slits fixed at the beam center) measured for beam currents of 40, 30, and 20 mA. The correlation is well pronounced at 40 mA, becomes less visible with a smaller beam current of 30 mA, and completely disappears at 20 mA. This measurement convincingly demonstrates that the observed correlation is created by the Coulomb forces within the distribution.

ISBN: 978-3-95450-194-6 ISSN: 2226-0366 doi:10.18429/JACoW-LINAC2018-FR1A01

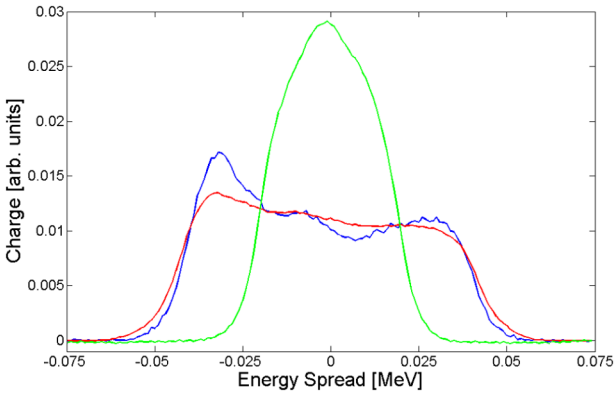

Figure 14: Plots of three different 1D partial projections on energy. Each plot has a different number of fixed slits near the center of the beam. The green curve fixes two slits, the red curve fixes three, and the blue curve fixes four. The curves are normalized by area.

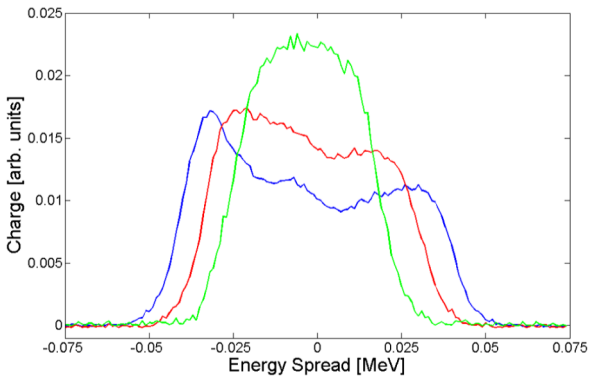

Figure 15: Plots of partial projections on energy with three different beam currents. The green curve is from 20 mA, the red curve is from 30 mA, and the blue curve is from 40 mA. The correlation is more pronounced with increasing current, which indicates Coulomb forces cause the correlation. The curves are normalized by area.

While a precise simulation using the measured distribution is left for future work, a simple computer simulation is sufficient to elucidate the beam physics. A 1 m long transport line consisting of drifts and four quadrupole magnets arranged similarly to the first 1 m of the BTF beam line was simulated using PARMILA particle-in-cell code [6]. An ideal 6D Gaussian function was used to generate the initial particle coordinates. Partial projections on the *w-y'* plane of the distribution function at the beam line exit are shown in Fig. 16 for two cases: a 10 mA and a 100 mA beam current. A pattern similar to the measurement in Fig. 10 is clearly visible only on the projection for high beam current, confirming that Coulomb forces are responsible for creating this correlation in the 6D phase space distribution. Furthermore, it is interesting to note that reproducing the correlation in simulation does not require any novel or complex beam physics. In parallel with the experiment, the key is knowing to look at the partial rather than the integrated 2D projection (e.g., to maintain a high dimensional approach when viewing the lower dimensional subspaces). This reinforces the notion that the full 6D distribution is required for a complete understanding of the beam physics.

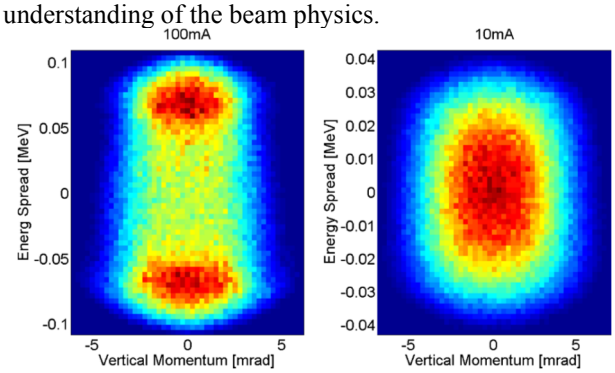

Figure 16: Two plots of the partial projection of the energy spread w against the vertical momentum y for a 100 mA (left) and a 10 mA (right) simulated beam transport.

The time required to complete a scan is the largest limiting factor for higher dimensionality scans. This limitation was partially diminished with the use of luminescent screens to measure the energy or the phase. Figure 17 shows a plan to significantly decrease scan time by removing the energy slit so that the two longitudinal dimensions can be completely measured simultaneously. In the future, we plan to add a FODO line to the end of the BTF with matching and mismatching quadrupoles to study beam halo development and benchmark simulations against the new measured distributions [7].

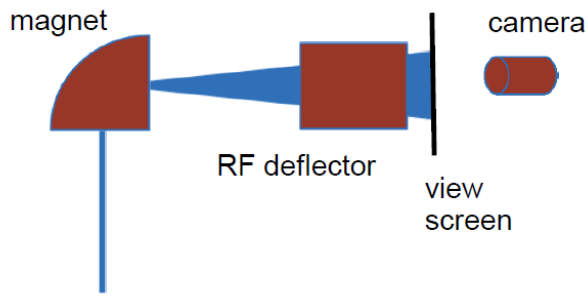

Figure 17: Proposed plan to measure the entire 2D longitudinal phase space simultaneously.

ACKNOWLEDGEMENT

This work has been partially supported by NSF Accelerator Science grant 1535312.

This manuscript has been authored by UT-Battelle, LLC, under Contract No. DE-AC0500OR22725 with the U.S. Department of Energy. The United States Government retains and the publisher, by accepting the article for publication, acknowledges that the United States Government retains a non-exclusive, paid-up, irrevocable, world-wide license to publish or reproduce the published form of this manuscript, or allow others to do so, for the United States Government purposes. The Department of Energy will provide public access to these results of federally sponsored research in accordance with the DOE Public Access Plan (http://energy.gov/downloads/doe-public-access-plan).

ISBN: 978-3-95450-194-6 ISSN: 2226-0366 doi:10.18429/JACoW-LINAC2018-FR1A01

REFERENCES

[1] S. Machida and R.D. Ryne, "Summary of session C: Space charge simulation and experiment," in *Proc. ICFA HB'04*, Bensheim, 2004, p. 454.

[2] J. Qiang, P.L. Colestock, D. Gilpatrick, H.V. Smith, T.P. Wangler, and M.E. Schulze, "Macroparticle simulation studies of a proton beam halo experiment," *PRSTAB*, vol. 5, no. 124201, 2002.

[3] A.V. Feschenko, "Methods and Instrumentation for Bunch Shape Measurements", in *Proc. PAC'01*, Chicago, IL, USA, Jun. 2001, pp. 517-519.

[4] A. Aleksandrov, M. Champion, M. Crofford, K. Ewald, Y. Kang, A. Menshov, M. Middendorf, S. Murry, R. Saethre, M. Stockli, A. Webster, R. Welton, A. Zhukov, "Status of the New 2.5 MeV Test Facility at SNS," in *Proc. LINAC'14*, Geneva, Switzerland, 2014, p. 1105.

[5] A. Zhukov et al., "Open XAL Status Report 2018," in *Proc. IPAC'18*, Vancouver, B.C., Canada, Apr.-May 2018, doi:10.18429/JACoW-IPAC2018-THPAK069

[6] J.H. Billen and H. Takeda, "PARMILA Manual", Los Alamos, NM. USA, 1998 Technical Report No. LAUR-98-4478 (revised 2004).

[7] Z. Zhang et al., "FODO Lattice Design for Beam Halo Research at SNS", presented at IPAC17, Copenhagen, Denmark, May 2017. doi.org/10.18429/JACoW-IPAC2017-TUPVA148